





ARTICLE

Characterizing Pattern of Topography and Geomorphology in the Hengduan Mountains, Southwest China

Youjun Chen ^{1,2,3*} , Yanying Chen ¹ , Xiaokang Hu ^{1,2,3} , Jianmeng Feng ^{1,2,3} 

¹ College of Agriculture and Biological Science, Dali University, Dali 671003, China

² Co-Innovation Center for Cangshan Mountain and Erhai Lake Integrated Protection and Green Development of Yunnan Province, Dali University, Dali 671003, China

³ Cangshan Forest Ecosystem Observation and Research Station of Yunnan Province, Dali University, Dali 671003, China

ABSTRACT

The Hengduan Mountains, situated on the southeastern edge of the Qinghai-Tibet Plateau, are the longest and widest north-south-oriented mountain range in China, exerting a significant influence on the ecological and geographical pattern. Understanding the topographic and geomorphological characteristics of the Hengduan Mountains is fundamental and crucial for research in related fields such as ecology, geography, and sustainability. In this study, Digital Elevation Model (DEM) data were utilized to extract and analyze the topography and geomorphology (TG) pattern. TG maps have been developed to quantitatively classify the TG types in the Hengduan Mountains by combining the five factors of elevation, slope, aspect, relief and landform. The spatial distribution and quantitative characteristics of these factors were mapped and investigated using geographic information systems. The results revealed that: (1) The Hengduan Mountains exhibit an elongated north-south distribution, with an average elevation of approximately 3746 m, an average slope of around 25°, and an average relief of about 266 m. (2) The Hengduan Mountains display significant elevation differences, with an overall high elevation, characterized by a trend of lower elevation in the east and higher elevation in the west, as well as irregular orientations of various aspects. (3) The 19 landform types were identified; the landform types of the Hengduan

*CORRESPONDING AUTHOR:

Youjun Chen, College of Agriculture and Biological Science, Dali University, Dali 671003, China; Co-Innovation Center for Cangshan Mountain and Erhai Lake Integrated Protection and Green Development of Yunnan Province, Dali University, Dali 671003, China; Cangshan Forest Ecosystem Observation and Research Station of Yunnan Province, Dali University, Dali 671003, China; Email: ecololv@163.com

ARTICLE INFO

Received: 16 September 2024 | Revised: 17 October 2024 | Accepted: 21 October 2024 | Published Online: 25 December 2024
DOI: <https://doi.org/10.30564/jees.v7i1.7300>

CITATION

Chen, Y., Chen, Y., Hu, X., et al., 2024. Characterizing Pattern of Topography and Geomorphology in the Hengduan Mountains, Southwest China. *Journal of Environmental & Earth Sciences*. 7(1): 414–422. DOI: <https://doi.org/10.30564/jees.v7i1.7300>

COPYRIGHT

Copyright © 2024 by the author(s). Published by Bilingual Publishing Group. This is an open access article under the Creative Commons Attribution-NonCommercial 4.0 International (CC BY-NC 4.0) License (<https://creativecommons.org/licenses/by-nc/4.0/>).

Mountains are primarily composed of low-relief high-mountains (42.0618%), low-relief mid-mountains (22.4624%), and high-elevation hills (20.5839%). The results of the study can provide data and information support for the ecology, environmental protection and sustainable development of the Hengduan Mountains.

Keywords: Topography; Geomorphology; Spatial Pattern; Digital Terrain Analysis; Hengduan Mountains

1. Introduction

Topography and geomorphology (TG) features reflect the physical surface characteristics and the processes that shape the Earth's morphology, making it one of the essential research areas in Earth science^[1–5]. TG patterns predominantly highlight the material transport, energy conversion, and dissipation processes occurring at the interfaces of the atmosphere, lithosphere, hydrosphere, and biosphere, exerting profound influences on geographical, ecological, and environmental elements, as well as human livelihood^[1, 5, 6]. TG attributes, such as elevation, slope, and relief^[7], affect the movement and flow of materials and energy within a specific landscape (e.g., nutrient cycling, sediment and pollutant transport) and influence the distribution and activities of organisms; simultaneously, these attributes are indispensable environmental elements for human production and life^[8], impacting decisions related to resource development and utilization strategies and ecological environmental protection programs. Comprehensively understanding the TG pattern of a region is fundamental and crucial for conducting related research^[9, 10], including environmental risk assessment, geomorphological hazards assessment (landslides, floods, soil erosion, etc.), landscape ecology, species distribution and evolution, and meteorology and climatology^[9, 11–13].

The rapid advancement of geographic information technology has provided new methods for mapping and analyzing TG feature^[14, 15]. Compared to traditional topographic maps, DEM offers high precision, convenient computation, and rapid visualization, making them the primary data source for TG feature research^[9, 16]. In recent years, scholars have conducted extensive research on TG features based on DEM data in various study areas, yielding fruitful research outcomes^[17–21].

The Hengduan Mountains are China's longest and widest north-south-oriented mountain system, serving as the boundary between the first and second terraces in China and the only region with both Pacific and Indian Ocean drainage

basins. It exerts a significant impact on China's ecological and geographical landscape. Influenced by the monsoons from both the Indian Ocean and the Pacific Ocean, the region's hydrothermal conditions are redistributed according to its TG variations. It is considered a typical mountainous ecological and geographical transition zone in southwestern China and an important climate-sensitive area. Situated in the upper and middle reaches of the Yangtze River, as well as the Mekong and Salween Rivers^[22], the Hengduan Mountains support multiple ecosystem services for these three major rivers and act as a crucial ecological barrier for downstream regions and the nation^[23]. The TG features affect the ecological and environmental patterns of the Hengduan Mountains. Exploring the TG features is necessary and important for a detailed understanding of the Hengduan Mountain resources and their ecological and environmental conditions. Meanwhile, analyzing the TG pattern in the Hengduan Mountains is of great significance for ecological conservation and restoration, maintaining biodiversity, soil and water conservation, and researching responses to global changes in the region.

However, there are still few systematic studies on the TG features in the Hengduan Mountains. In this work, we focus on a detailed analysis of the TG pattern in the Hengduan Mountains. Employing DEM data and geographic information system (GIS) technology, we mapped five TG factors in the Hengduan Mountains and analyzed their spatial pattern. The research aims to provide detailed and reliable foundational TG data, with a view to providing a basis and scientific reference for the compilation of topographic and geomorphologic maps, quantitative evaluation of the ecological environment, and sustainable development in the Hengduan Mountains.

2. Study Area

The Hengduan Mountains are located in southwestern China and represent a typical north-south-oriented mountain

system^[23]. Within this region, north-south-oriented mountain ranges and deep valleys are interspersed, featuring a total of seven parallel mountain ranges and six major rivers (as shown in **Figure 1**). The Hengduan Mountains are high in the north and low in the south and display a distinctive vertical zonation of vegetation and climate.

The mutual extrusion of the Eurasian continental plate by the Indian subcontinent plate led to the dramatic uplift of the Hengduan Mountains, making it one of the tightest extruded and narrowest composite orogenic belts in the world. At the same time, due to the combined effects of glacier melting and river erosion, valleys with large elevation differences have been formed.

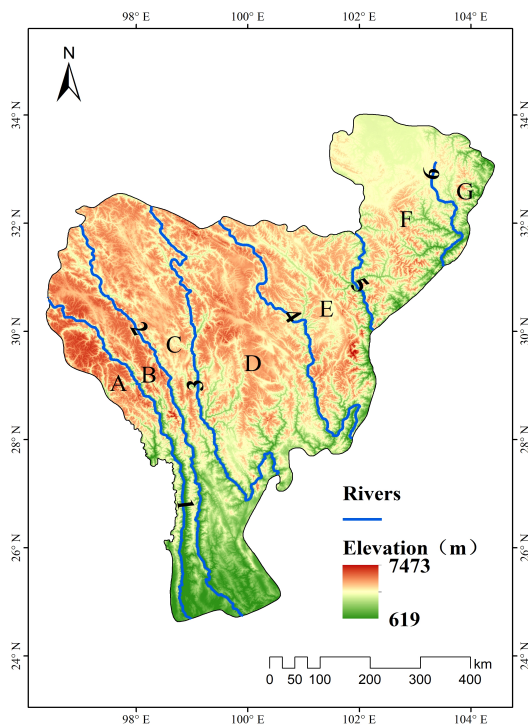


Figure 1. Distribution of mountain ranges and rivers in the Hengduan Mountains.

Note: 1 is the Nujiang River; 2 is the Lancang River; 3 is the Jinsha River; 4 is the Yalong River; 5 is the Dadu River; 6 is the Minjiang River. A represents the Boshulaling-Gaoligong Mountains; B represents the Tiantaweng-Nushan Mountains; C represents the Mangkang-Yunling Mountains; D represents the Shaluli Mountains; E represents the Daxue-Gongga Mountains; F represents the Qionglai Mountains; G represents the Minshan Mountains.

3. Materials and Methods

3.1. Data Sources

The study utilized ASTER Global Digital Elevation Model (GDEM) Version 3 as the foundational data. ASTER GDEM Version 3 is a data product generated using all

ASTER Level 1A archive data acquired between March 1, 2000, and November 30, 2013. It has a spatial resolution of 1 arcsecond and covers a region from North Latitude 83° to South Latitude 83°^[1]. The data is distributed in standard GeoTIFF format through the USGS LPDAAC database (<https://lpdaac.usgs.gov/data/>).

3.2. Methods

Topographic analysis is a prerequisite for geomorphic regionalization. For the study area with complex geomorphology, several key parameters were selected to characterize the topography and geomorphology. These parameters include elevation, slope, aspect, relief, and landform. Firstly, graded raster maps of elevation, slope, and aspect were generated from the GDEM by using QGIS tools (Raster analysis and Raster terrain analysis). Landform refers to the surface morphology characterized by variations in elevation and relief^[24, 25]. Therefore, the landform pattern can be obtained by overlaying elevation and relief classification data. However, mapping relief is a more intricate process.

Relief refers to the difference in elevation between the highest and lowest points within a “specific extent”^[26]. Relief varies with the location and extent of different study areas, with obvious scale and regional effects. Thus, for a given study area, the calculation of relief should first determine the size of the analysis grid in that region^[27]. The “specific extent” mentioned previously refers to the optimal size of the analysis grid for the calculation of relief for the given study area. Therefore, the determination of the optimal grid size becomes crucial for mapping the relief in the Hengduan Mountains. The process of calculating the optimal grid size for the relief in the study area is outlined as follows:

1. Using the neighborhood analysis function, elevation maximum and minimum values within an $n \times n$ grid ($n = 2, 3, 4, \dots, 50$) were quantified. The difference between the maximum and minimum elevations represents the relief within the $n \times n$ grid.
2. Based on the relief within the $n \times n$ grid, we computed the maximum relief values for the entire study area at the $n \times n$ grid. Additionally, we calculated the average relief values for the entire study area at the $n \times n$ grid. The results are shown in **Table 1**.
3. Based on the data obtained from **Table 1**, we employed

Equation (1) to calculate the terrain magnitude sequence T_n (relief per unit area) within each analysis unit ($n \times n$ grid). Then, we employed the mean change point analysis^[28] to identify the threshold point at which the relief transitions from increasing to leveling off^[29, 30].

$$T_n = t_n / s_n (n = 2, 3, 4, 5, \dots, 50) \quad (1)$$

In the equation, T_n represents the relief degree within the analysis unit; t_n represents the average relief within the analysis unit; s_n represents the area of the grid cell within the analysis unit, and n is the sequence number of the grid.

Taking the natural logarithm ($\ln(T_n)$) of the T_n results in the sequence Y , where $Y = y_i, i = 1, 2, 3, 4, 5, \dots, 49$. Calculating the arithmetic mean \bar{Y} and the sum of squared deviations S ($S = 31.17$) for the Y sequence; dividing Y into two subseries: y_1, y_2, \dots, y_i and y_{i+1}, \dots, y_{49} , and calculating the difference in the sum of squared deviations between

the two segments S_i . Plotting the variation curve (Figure 2) of the difference between S and S_i , it can be seen that the difference between S and S_i reaches its maximum at the grid size of 17×17 , which leads to the grid size of 17×17 (approximately $265,433.10 \text{ m}^2$) as the best statistical unit. Such, relief information for the Hengduan Mountains will be extracted at a grid size of 17×17 .

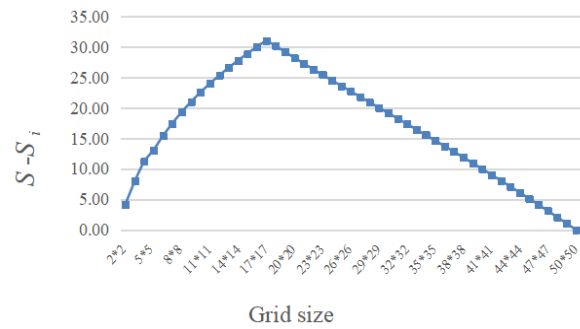


Figure 2. Relation between size of analysis grid and $S-S_i$.

Table 1. Relief amplitude changing with analysis grid size in Hengduan mountains.

Grid Size	2*2	3*3	4*4	5*5	6*6	7*7	8*8	9*9	10*10
Grid area/m ²	3,673.81	8,266.08	14,695.26	22,961.34	33,064.33	45,004.23	58,781.03	74,394.74	91,845.36
Maximum relief/m	411	613	768	252	941	976	1,016	1,059	1,107
Average relief/m	19.48	38.20	56.35	27.77	91.15	107.84	124.08	139.90	155.33
Grid Size	11*11	12*12	13*13	14*14	15*15	16*16	17*17	18*18	19*19
Grid area/m ²	111,132.89	132,257.32	155,218.66	180,016.91	206,652.07	235,124.13	265,433.10	297,578.98	331,561.76
Maximum relief/m	1,149	1,218	1,317	1,401	1,484	1,536	1,578	1,613	1,648
Average relief/m	170.38	185.09	199.45	213.50	227.23	240.68	253.85	266.75	279.40
Grid Size	20*20	21*21	22*22	23*23	24*24	25*25	26*26	27*27	28*28
Grid area/m ²	367,381.45	405,038.05	444,531.56	485,861.97	529,029.29	574,033.52	620,874.66	669,552.70	720,067.65
Maximum relief/m	1,692	1,728	1,775	1,825	1,869	1,901	1,933	1,977	2,003
Average relief/m	291.80	304.00	315.90	327.62	339.13	350.44	361.55	372.48	383.23
Grid Size	29*29	30*30	31*31	32*32	33*33	34*34	35*35	36*36	37*37
Grid area/m ²	772,419.51	826,608.27	882,633.94	940,496.52	1,000,196.01	1,061,732.40	1,125,105.70	1,190,315.91	1,257,363.03
Maximum relief/m	2,031	2,064	2,096	2,126	2,150	2,178	2,208	2,242	2,268
Average relief/m	393.80	404.20	414.44	424.52	434.45	444.23	453.87	463.37	472.73
Grid Size	38*38	39*39	40*40	41*41	42*42	43*43	44*44	45*45	46*46
Grid area/m ²	1,326,247.05	1,396,967.98	1,469,525.82	1,543,920.56	1,620,152.21	1,698,220.77	1,778,126.24	1,859,868.61	1,943,447.89
Maximum relief/m	2,301	2,326	2,345	2,356	2,361	2,361	2,361	2,361	2,361
Average relief/m	481.97	491.07	500.06	508.92	517.67	526.29	534.82	543.23	551.55
Grid Size	47*47	48*48	49*49	50*50					
Grid area/m ²	2,028,864.08	2,116,117.18	2,205,207.18	2,296,134.09					
Maximum relief/m	2,368	2,384	2,398	2,406					
Average relief/m	559.75	567.87	575.87	583.80					

4. Results

4.1. Topographic Pattern

Elevation and relief are key indicators that visually reflect the structural characteristics of the regional TG, and they are also important bases for determining the landform types and dividing the geomorphological units of the region.

Referring to the Chinese digital landform classification criteria^[31, 32], elevation was categorized into four levels (Table 2, Figure 3a), and relief of the Hengduan Mountains was categorized into five classes (Table 3, Figure 3b). As indicated in Table 2, the Hengduan Mountains generally exhibit higher elevation, with 67.0095% of its terrain situated above 3,500 m. There are virtually no areas with elevation below 1,000 m throughout the region (comprising only 0.1678%

of the total area). Regions with extremely high elevation (>5,000 m) occupy nearly 3% of the area. The elevation patterns of the Hengduan Mountains display a strip-like distribution characterized by higher elevation in the north and lower elevation in the south, as well as higher elevation in the west and lower elevation in the east.

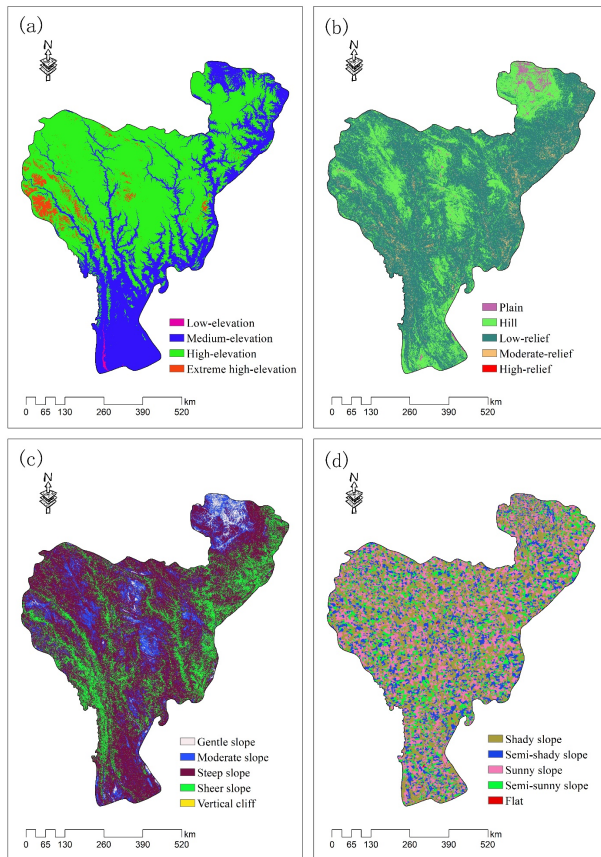


Figure 3. Maps of the topographic distribution pattern in the Hengduan Mountains show: (a) elevation classification distribution, (b) relief classification distribution, (c) slope classification distribution, and (d) aspect classification distribution.

Many geoscientists, resource scientists and environmental scholars have taken the relief as an important indicator for regional resource and environmental evaluation, and as one of the key indicators for soil erosion sensitivity, freeze-thaw erosion sensitivity, geological environment, and ecological environment evaluation. From **Figure 3b**, it can be observed that the relief in the Hengduan Mountains is generally significant, with a maximum relief of 1610 m and an average relief of 266 m. The statistical information in **Table 3** reveals that, as a high-altitude plateau region, the relative heights in the Hengduan Mountains are mainly in the range of >30–500 m, accounting for 95.4701%. The

predominant relief type is low-relief, constituting 66.7691%. These are primarily concentrated on the east and west sides and in the central region.

Slope and aspect mainly affect the spatial differentiation of moisture and temperature, and have important reference value for regional soil erosion control measures. Considering the Commission for the Geological Map of the World (CGMW) criteria for the classification of slope and the actual conditions of the study area, the slope was divided into five categories (**Table 4**). As shown in **Table 4** and **Figure 3c**, steep slope dominates the Hengduan Mountains, accounting for the largest proportion at 64.2248%, followed by sheer slope at 20.74%. Both of these categories exhibit a ribbon-like distribution within the study area.

The study area's aspect was categorized into five fundamental directions (**Table 5**). Due to its extensive geographical range and complex mountainous terrain with various geological structures, these aspects are intermixed without clear zonal patterns (as shown in **Figure 3d**). The primary aspect types are sunny slope and shady slope, accounting for 29.4100% and 36.2703%, respectively (**Table 5**). There is almost no flat terrain distribution, making up a minimal percentage of only 0.0495%.

The topographic factors such as elevation, relief, and slope of the Hengduan Mountains exhibit a banded distribution pattern (**Figure 3**), which is basically consistent with the tectonic orientation of the region. The central part is oriented in a north-south direction, while the northwest part is oriented from northwest to nearly east-west. The diverse distribution patterns of altitude, relief, and slope have created typical terrain features of high mountains, deep valleys, and large elevation differences. The Hengduan Mountains are distributed side by side from east to west, with mountains and rivers alternating. Among them, the Jinsha River, Lancang River, and Nujiang River (also known as the Three Rivers) are closest to each other near latitude $27^{\circ}30'N$, with a straight-line distance of only 76 kilometers (**Figure 1**); the three rivers are narrow and steep on both sides, and belong to a typical "V"-shaped deep canyon. The terrain features of high mountains and deep valleys have had a huge impact on the climate, vegetation distribution, and rivers in the Hengduan Mountains, such as the formation of numerous dry and hot river valleys, as well as narrow and deep river channels with large drops in the region.

Table 2. Elevation classifications and their percentage in the Hengduan Mountains.

Elevation Classification	Range/m	Percentage/%	Cumulative Percentage/%
Low-elevation	≤1000	0.1678	0.1678
Medium-elevation	>1000–3500	32.8227	32.9905
High-elevation	>3500–5000	64.0282	97.0187
Extreme high-elevation	>5000	2.9813	100

Table 3. Relief classifications and their percentage in the Hengduan Mountains.

Relief Classification	Range/m	Percentage/%	Cumulative Percentage/%
Plain	≤30	1.5296	1.5296
Hill	>30–200	28.7010	30.2306
Low-relief	>200–500	66.7691	96.9997
Moderate-relief	>500–1000	2.9981	99.9978
High-relief	>1000–2500	0.0022	100.0000

Table 4. Slope classifications and their percentage in the Hengduan Mountains.

Slope Classification	Angle Range/°	Percentage/%	Cumulative Percentage/%
Gentle slope	0–5	2.1357	2.1357
Moderate slope	>5–15	12.7146	14.8502
Steep slope	>15–35	64.2248	79.0750
Sheer slope	>35–55	20.7400	99.8151
Vertical cliff	>55–90	0.1849	100.0000

Table 5. Aspect classifications and their percentage in the Hengduan Mountains.

Aspect Classification	Angle Range/°	Percentage/%	Cumulative Percentage/%
Flat	–1	0.0495	0.0495
Shady slope	0–45 & >315–360	36.2703	36.3198
Semi-shady slope	>45–135	18.5427	54.8625
Sunny slope	>135–225	29.4100	84.2725
Semi-sunny slope	>225–315	15.7275	100.0000

4.2. Landform Pattern

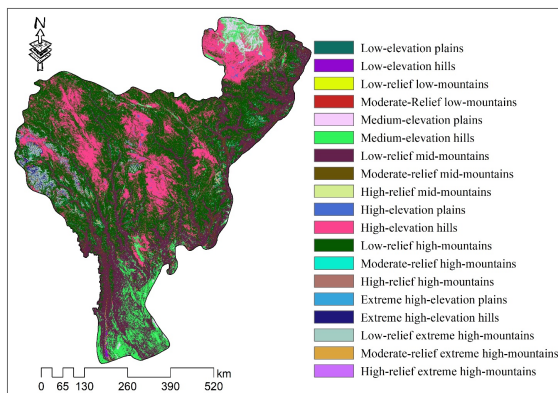
Studying the types and patterns of landforms in the Hengduan Mountains can provide geomorphological support for resource and environmental management, ecological and biodiversity research, and ecological governance. Referring to the Chinese digital landform classification system^[31, 32], the landform of the Hengduan Mountains was divided into 19 categories (**Figure 4, Table 6**).

The primary landform in the Hengduan Mountains is low-relief high-mountains, accounting for 42.0618%. They are distributed in a strip-like pattern in the central and western regions. Low-relief mid-mountains and high-elevation hills also have relatively high proportions, at 22.4624%

and 20.5839%, respectively. Low-relief mid-mountains are mainly distributed in the southern region and the eastern side, while high-elevation hills have a sheet-like distribution in the central and northeastern areas. Medium-elevation hills are mainly found in the southern region, accounting for 7.3418%. Low-relief extreme high-mountains cover a smaller proportion, at 2.1874%, primarily distributed on the western edge, with scattered occurrences in the central and eastern regions. Moderate-relief mid-mountains have sporadic distribution on both the eastern and western sides (1.8564%). Medium-elevation plains are mainly found in the northeastern part (1.2023%). The remaining geomorphological types each occupy less than 1.00% of the total area, and their distribution is highly fragmented.

Table 6. Landform types and their percentage in the Hengdun Mountains.

Geomorphological Types	Elevation Range/m	Relief Range/m	Percentage/%	Cumulative Percentage/%
Low-elevation plains	≤1000	≤30	0.0035	0.0035
Low-elevation hills	≤1000	>30–200	0.1071	0.1106
Low-relief low-mountains	≤1000	>200–500	0.0574	0.1680
Moderate-relief low-mountains	≤1000	>500–1000	0.0005	0.1685
Medium-elevation plains	>1000–3500	≤30	1.2023	1.3708
Medium-elevation hills	>1000–3500	>30–200	7.3418	8.7126
Low-relief mid-mountains	>1000–3500	>200–500	22.4624	31.175
Moderate-relief mid-mountains	>1000–3500	>500–1000	1.8564	33.0314
High-relief mid-mountains	>1000–3500	>1000	0.0015	33.0329
High-elevation plains	>3500–5000	≤30	0.3237	33.3566
High-elevation hills	>3500–5000	>30–200	20.5839	53.9405
Low-relief high-mountains	>3500–5000	>200–500	42.0618	96.0023
Moderate-relief high-mountains	>3500–5000	>500–1000	1.0282	97.0305
High-relief high-mountains	>3500–5000	>1000	0.0004	97.0309
Extreme high-elevation plains	>5000	≤30	0.0002	97.0311
Extreme high-elevation hills	>5000	>30–200	0.6682	97.6993
Low-relief extreme high-mountains	>5000	>200–500	2.1874	99.8867
Moderate-relief extreme high-mountains	>5000	>500–1000	0.1130	99.9997
High-relief extreme high-mountains	>5000	>1000	0.0003	100.0000

**Figure 4.** Map of the distribution of landform types in the Hengdun Mountains.

5. Conclusions

This study explores the TG features of the Hengdun Mountains based on quantitative indicators such as elevation, relief, slope, aspect, as well as landform classification. The results not only lay a foundation for the scientific evaluation of the TG features of the Hengdun Mountains, but also provide support for the ecological and environmental protection and sustainable development of the Hengdun Mountains. The main conclusions are as follows:

1. Using the mean change point analysis, we determined that the optimal analysis scale for relief in the Hengdun Mountains is approximately 265,433.10 m². In the study area, there is no extensive distribution of highly undulating mountainous terrain, and the predominant relief type is small undulating mountainous terrain, concentrated on the eastern

and western sides and in the central region.

2. The Hengdun Mountains exhibit a long and narrow north-south distribution, with an average elevation of approximately 3,746 m, an average slope of about 25°, and an average relief of approximately 266 m. The mountains have significant elevation variations, showing a pattern of higher elevations in the north and lower elevations in the south, as well as higher elevations in the west and lower elevations in the east. The overall elevation is relatively high, with 67.0095% of the mountain areas exceeding 3,000 m in elevation. Steep slopes (>15°–35°) cover the largest area in the study region, followed by sheer slopes (>35°–55°), and these two categories exhibit a ribbon-like distribution.

3. Based on elevation and relief, we identified 19 landform types. Low-relief high-mountains (42.0618%), low-relief mid-mountains (22.4624%), and high-elevation hills (20.5839%) are the main landform types. High-relief mid-mountains, high-relief high-mountains, and high-relief extreme high-mountains account for only 0.0022% of the total area in the entire region.

In recent years, the application of TG information has become more and more extensive, and the mining and in-depth application of this information also deserves attention. We will introduce variables such as population, ecological and environmental factors to improve the understanding of the impact of the TG features on the population, ecology and environment, and to promote the protection and restoration of the ecological environment as well as the green and sustainable development in the Hengdun Mountains.

Author Contributions

All authors cooperated with the research idea and methodology. Data gathering and analysis: Y.C. (Yanying Chen), and Y.C. (Youjun Chen); writing original draft preparation: Y.C. (Youjun Chen); writing review and editing: Y.C. (Youjun Chen), X.H., and J.F.; visualization: Y.C. (Yanying Chen); supervision: Y.C. (Youjun Chen). All authors have read and agreed to the published version of the manuscript.

Funding

This research was funded by the Yunnan Provincial Basic Research Joint Special Fund Project (2019FH001(-052)) and Cangshan Mountain Synthetic Scientific Expeditions Fund.

Institutional Review Board Statement

Not applicable.

Informed Consent Statement

Not applicable.

Data Availability Statement

The data supporting of this study are available from the corresponding authors, upon reasonable request.

Acknowledgments

We are grateful to the anonymous reviewers whose constructive suggestions have improved the quality of this study. We thank to the Innovative Team of Plant Ecology and Climate Change in Hengduan Mountains and the Plant Ecology Innovation Team of Dali University for their help.

Conflicts of Interest

The authors declare no conflict of interest.

References

- [1] Szypuła, B., 2017. Hydro-Geomorphology - Models and Trends. Intech Open: Zagreb, Croatia. pp. 1–122.
- [2] De Jong, M.G.G., Sterk, H.P., Shinneman, S., et al., 2021. Hierarchical geomorphological mapping in mountainous areas. *Journal of Maps*. 17, 214–224.
- [3] Kazemi Garajeh, M., Feizizadeh, B., Weng, Q., et al., 2022. Desert landform detection and mapping using a semi-automated object-based image analysis approach. *Journal of Arid Environments*. 199, 104721.
- [4] Quesada-Román, A., Peralta-Reyes, M., 2023. Geomorphological mapping global trends and applications. *Geographies*. 3(3), 610–621.
- [5] Bishop, M.P., James, L.A., Shroder, J.F., et al., 2012. Geospatial technologies and digital geomorphological mapping: Concepts, issues and research. *Geomorphology*. 137, 5–26.
- [6] Wang, D., Laffan, S.W., Liu, Y., et al., 2010. Morphometric characterisation of landform from DEMs. *International Journal of Geographical Information Science*. 24, 305–326.
- [7] Saha, S., Paul, G.C., Hembram, T.K., 2019. Classification of terrain based on geo-environmental parameters and their relationship with land use/land cover in Bansloi River basin, Eastern India: RS-GIS approach. *Applied Geomatics*. 12, 55–71.
- [8] Barbălată, L., Comănescu, L., 2021. Environmental sustainability and the inclusion of geomorphosites in tourist activity—case study: The Baiului Mountains, Romania. *Sustainability*, 13(14), 8094.
- [9] Zangana, I., Otto, J.-C., Mäusbacher, R., et al., 2023. Efficient geomorphological mapping based on geographic information systems and remote sensing data: An example from Jena, Germany. *Journal of Maps*. 19(1), 2172468.
- [10] Ferrando, A., Bosino, A., Bonino, E., et al., 2023. Geomorphology and geoheritage in the Piana Crixia Natural Park (NW Italy). *Journal of Maps*. 19(1), 2257731.
- [11] Garcia, G.P.B., Grohmann, C.H., 2019. DEM-based geomorphological mapping and landforms characterization of a tropical karst environment in southeastern. *Brazil Journal of South American Earth Sciences*. 93, 14–22.
- [12] Bollati, I.M., Cavalli, M., 2021. Unraveling the relationship between geomorphodiversity and sediment connectivity in a small alpine catchment. *Transactions in GIS*. 25(5), 2481–2500.
- [13] Coratza, P., Bollati, I.M., Panizza, V., et al., 2021. Advances in geoheritage mapping: Application to iconic geomorphological examples from the Italian landscape. *Sustainability*. 13(20), 11538.
- [14] Na, J., Ding, H., Zhao, W., et al., 2021. Object-based large-scale terrain classification combined with segmentation optimization and terrain features: A case study in China. *Transactions in GIS*. 25, 2939–2962.
- [15] Bufalini, M., Materazzi, M., De Amicis, M., et al., 2021. From traditional to modern ‘full coverage’ geomorphological mapping: A study case in the Chienti

- river basin (Marche region, central Italy). *Journal of Maps*. 17, 17–28.
- [16] Ngunjiri, M.W., Libohova, Z., Owens, P.R., et al., 2020. Landform pattern recognition and classification for predicting soil types of the Uasin Gishu Plateau, Kenya Catena. *CATENA*. 188, 104390.
- [17] Brigham, C.A.P., Crider, J.G., 2022. A new metric for morphologic variability using landform shape classification via supervised machine learning. *Geomorphology*. 399, 108065.
- [18] Sărășan, A., Józsa, E., Ardelean, A.C., et al., 2018. Sensitivity of geomorphons to mapping specific landforms from a digital elevation model: A case study of drumlins. *Area*. 51, 257–267.
- [19] Yang, X., Tang, G., Meng, X., et al., 2019. Classification of karst Fenglin and Fengcong landform units based on spatial relations of terrain feature points from DEMs. *Remote Sensing*. 11(16), 1950.
- [20] Xu, Y., Zhu, H., Hu, C., et al., 2021. Deep learning of DEM image texture for landform classification in the Shandong area, China. *Frontiers of Earth Science*. 16, 352–367.
- [21] Li, S., Xiong, L., Tang, G., et al., 2020. Deep learning-based approach for landform classification from integrated data sources of digital elevation model and imagery. *Geomorphology*. 354, 107045.
- [22] Wang, Y., Dai, E., Yin, L., et al., 2018. Land use/land cover change and the effects on ecosystem services in the Hengduan Mountain region, China. *Ecosystem Services*. 34, 55–67.
- [23] Chen, T., Peng, L., Wang, Q., et al., 2017. Measuring the coordinated development of ecological and economic systems in Hengduan Mountain area. *Sustainability*. 9(8), 1270.
- [24] Janowski, L., Tylmann, K., Trzcinska, K., et al., 2022. Exploration of glacial landforms by object-based image analysis and spectral parameters of digital elevation model. *IEEE Transactions on Geoscience and Remote Sensing*. 60, 1–17.
- [25] Zhang, B., Fan, Z., Du, Z., et al., 2020. A geomorphological regionalization using the upscaled DEM: the Beijing-Tianjin-Hebei area, China case study. *Scientific Reports*. 10, 10532.
- [26] Montgomery, D.R., Brandon, M.T., 2002. Topographic controls on erosion rates in tectonically active mountain ranges. *Earth and Planetary Science Letters*. 201, 481–489.
- [27] Xiong, L., Tang, G., Yang, X., et al., 2021. Geomorphology-oriented digital terrain analysis: Progress and perspectives. *Journal of Geographical Sciences*. 31, 456–476.
- [28] Shirvani, A., 2015. Change point analysis of mean annual air temperature in Iran. *Atmospheric Research*. 160, 91–98.
- [29] Liu, S., Cui, Y., Lu, F., et al., 2013. The analysis of relief amplitude in Qinghai Province based on GIS. *Proceedings of the 21st International Conference on Geoinformatics*; Kaifeng, China, 20–22 June 2013. pp. 1–5.
- [30] Yang, S.-m., Zhang, Y.-h., Chen, S., 2018. Extraction of terrain relief amplitude based on GIS and change point theory. *DEStech Transactions on Computer Science and Engineering*. DOI: <https://doi.org/10.12783/dtcse/pcmm2018/23712>
- [31] Cheng, W., Zhou, C., Chai, H., et al., 2010. Quantitative extraction and analysis of basic morphological types of land geomorphology in China. *Geo-information Science*. 11, 725–736.
- [32] Zhu, H., Xu, Y., Cheng, Y., et al., 2019. Landform classification based on optimal texture feature extraction from DEM data in Shandong Hilly Area, China. *Frontiers of Earth Science*. 13, 641–655.